Electron Cooling and Accumulation Results at 200 MeV

T. Ellison, W. Kells, V. Kerner, F. Mills,
R. Peters, T. Rathbun, D. Young
Fermi National Accelerator Laboratory
Batavia, Illinois 60510

P.M. McIntyre
Texas A&M University
College Station, Texas 77843

Abstract

A description is presented of the highest energy, to date, electron cooling studies (200 MeV protons cooled by 111 KeV electron beam). Results on equilibrium proton distributions, damping times, and longitudinal friction force are presented. Preliminary investigation of stacking and coalescing successive single turn proton injection batches into a cold core is reported.

1. Introduction

The electron cooling of ion beams confined in storage rings, first demonstrated by the Novosibirsk group,[1] has been studied at Fermilab as a means to cool and accumulate $\bar{p}$ target secondaries. This method has the potential of providing the highest possible luminosity beams for ultra high energy $\bar{p}p$ collisions (such as the Fermilab ED/S).[2] Here we describe the cooling of proton beams produced by the Fermilab linac (fixing the kinetic energy of this work $\equiv$ 200 MeV/c^2) and degraded ("heated") to provide a large emittance beam to simulate $\bar{p}$ accumulation conditions. Both the storage ring and electron cooler were designed to function (with possible modifications) as the accumulator components for a working HEP $\bar{p}$ source. Thus key parameters of the cooler derive from the need to "match" to the existing Fermilab complex (e.g. emittance, location, energy, circumference, cycle time, etc.). In particular the electron cooling beam is typically run at much higher power (designed for 28 ampere ~200 kV operation). than has been previously attempted.[3]

Both the ring and electron device as well as their planned $\bar{p}$ accumulation use have been previously described.[4] Here we report the actual cooling data measured at 200 MeV (as well as some initial data taken at 114 MeV)[5] along with an interpretation and comparison with oter existant results. Emphasis in these studies was on parameters directly relating to momentum cooling and momentum stacking of large initial phase space ion beams (the mode of accumulation natural to the electron cooling method). These include: cooled/uncooled beam lifetimes; longitudinal friction

force, equilibrium ion emittances; accretion of fresh protons into an existant cold core ("stacking").

A natural notation is used where $\vec{v}_{p,e}$ = proton, electron velocity in the mean moving frame and $\vec{u} \equiv \vec{v}_p - \vec{v}_e$. As a guide we recall the basic ($B_z = 0$, $v_p > \sqrt{m/M}\, v_e$) expression for the friction force experienced by the protons moving through an electron distribution $f(\vec{v}_e)$.[6]

$$dF = -\frac{4\pi e^4 n}{M}\frac{\vec{u}}{|\vec{u}|^3} L(u)\, f(\vec{v}_e) d^3 v_e$$

where L is the relevant Coulomb logarithm. Unless otherwise stated we use (e.g. F) moving frame quantities.

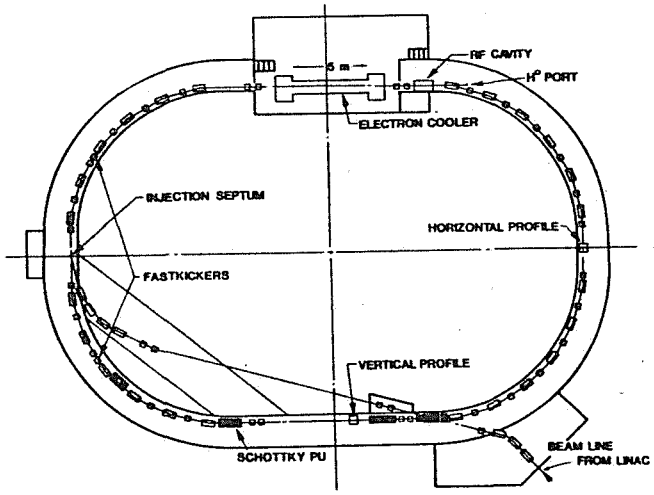

FIG. 1. Plan view of electron cooling ring (ECR). Open rectangles are bends; small open squares are quadrupoles (FODO structure)

2. Electron Cooling Ring (ECR) and Diagonstics

The design strategy of the storage synchrotron (figure 1) was to incorporate compactness and large phase space acceptance (i.e. strong focusing) along with low dispersion (for simultaneous cooling at different momenta with a minmum diameter e^- beam); high β_c function (to minimize v_p where frictional force $\propto \vec{v}_p/v_p^3$ for $|\vec{v}_p| > |\vec{v}_e|$); and [2] long straight sections (allowing large ζ).[7] The actual nominal operating parameters are given in Table I (for 114 MeV run parameters see Ref. 5).

TABLE I. Parameters of the electron cooling ring (ECR) and electron beam during cooling experiments with symbols used in text indicated.

PARAMETER	VALUE (units)
Relativistic parameters β,γ	0.57, 1.21
Revolution period, T_o	0.798 μsec.
Effective radius	21.56 m
Bend field	4.29 k gauss
γ_T, η	3.68, 0.609
Tunes, $\nu_{V,H}$	5.42, 3.68
Acceptance, $\epsilon_{H,V}$	20π, 40π mm-mrad
Beta functions at cooler (β_oV,H)	25 m, 20 m
e^- cathode potential V_o	-111 KeV
e^- current (I_e); e^- density (n) $0.75\text{-}5.0\times10^{-7}$cm^{-3}	0.5-4amp;
Interaction length; fraction (ζ)	5 m; 0.037
e^- beam radius	2.5 cm
Solenodial guide field (B_z)	930 gauss
Cooling region vacuum (2 amp)	$\gtrsim 5\times10^{-9}$ Torr
Mean ring vacuum (e^- off)	$\lesssim 2\times10^{-10}$ Torr

The lattice has natural 4 fold symmetry, broken only by the electron guide solenoid (tune shift = 0.0045) and the electron beam space charge Successful running was accomplished close enough to the "coupling resonance" (equal fractional ν_V, ν_H) that the marked V/H solenoid coupling could be studied.

The extreme ion beam conditions possible in electron cooling place unique demands on diagnostics. All cooling experiments to date have had diagnostic limited data in some respects, with their strong points complimentary. However, this situation has made data difficult to compare due to the diverse machine parameters. Besides traditional accelerator physics diagnostics ("wires" scanned accross the aperture; scintillator loss monitors; RF resonant knock outs; intercepting profile wire chambers, etc.) we developed several novel non destructive techniques.

The highest intensity routinely injected into our ring (limited by radiation safety) was 0.40μA (2×10^6 protons). High sensitivity, slow wave (taking advantage of our $\beta \sim 1/2$) Schottky pick ups were exclusively used to monitor δp/p and measure tunes.[9] Much higher real time sensitivity was possible by RF bunching the beam (which distorts and complicates the cooling dynamics but is ideal for intensity monitoring). Much less sensitive transversly split pick up pairs (one in each quadrupole) were employed as monitors of the horizontal closed orbit position. A similar but doubly split (giving horizontal and vertical displacement information) pick up was installed contiguously with the ends of the 5 m electron interaction region. By signal comparison, this allowed alignment of the proton and electron beam charge centers of gravity.

"Profilometers" directly measured coasting beam projected density by position sensitive counting of ions formed by beam-gas collisions which were swept perpendicularly out of the aperture by a transverse DC electric field.[10] The position sensitive counter consisted of a two stage 8 x 10 cm MCP proximity focused onto a resistive sheet charge division network. Profiles consisted of 512 ionization events digitally reconstructed into scatter plots or histograms. Resolution of the device was digital LSB limited (8 bit ADC's) and measured to be $\lesssim$ 0.2 mm. The "frame" rate depends on local residual gas density at the monitor up to a digitization rate limitation of ~100 Hz. When good temporal resolution was essential (e.g. to follow transverse cooling evolution) or beam intensity was low, a local piezoelectric valve "puffed" H_2 into the aperture.

Finally, limited neutral hydrogen recombination rate information was obtained by "observing" the interaction section through a thin window with a coinadence/ranging scintillation counter teleoscope.

The electron system is illustrated in figure 2.[11] An energy recuperating design is employed which was remarkably successful: typically δI/I loss with ($\lesssim$ 3 ampere beam current) was only a few $\times 10^{-4}$ (we have achieved 1.0×10^{-5} loss $\lesssim$ 2.0 ampere). We credit the unique immersed |B| design of the deceleration column/collector for this performance. The system vacuum and loss

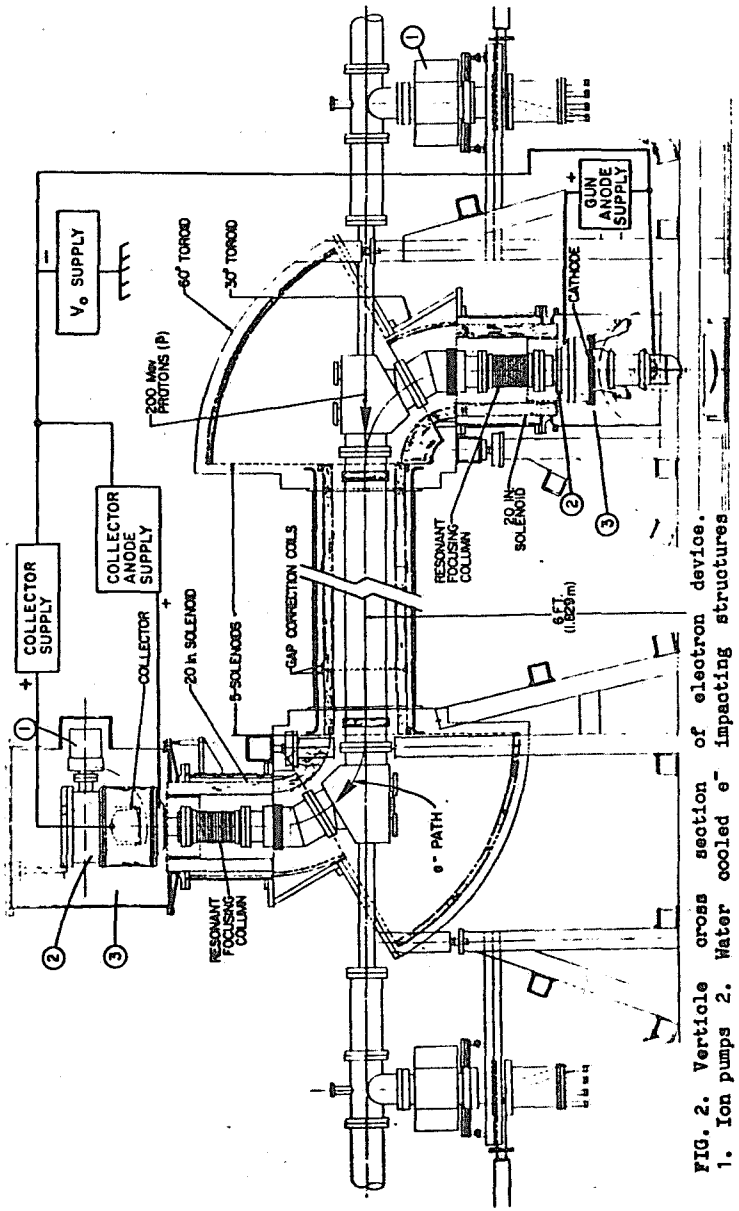

FIG. 2. Vertiole cross section of electron device.
1. Ion pumps 2. Water cooled e⁻ impacting structures
3. SF_6 insulated volumes.

FIG 2 (FULL PAGE)

characteristics are partially summarized in figure 3, which shows a residual vacuum pressure above the cold system value ($\simeq 4 \times 10^{-10}$T). We attribute this to the unpumped cathode leg (unbaked as well, in contrast to the hard baked interaction region) being outgassed by the 1100°C cathode.

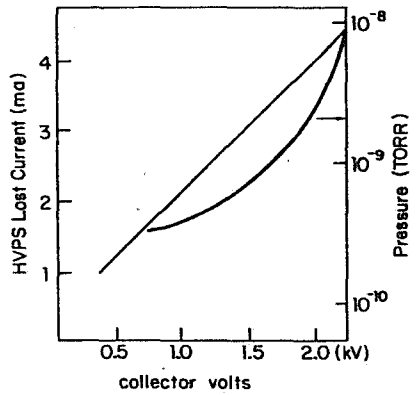

FIG. 3. Vacuum in cooling region as a function of collector anode potential above cathode potential.

A convergent Pierce gun design was chosen (area convergence ratio = 6.25) to accommodate the high beam currents needed for fast FNAL booster matched, accumulation. Convergence, however, leads to an adiabadic increase T_c (electron temperature at the cathode: 1100°C ≡ 0.11 ev) to $T_{e\perp} = 6.25\ \gamma^2 T_c = 1.01$ ev (interaction region, moving frame transvence electron temperature). Much larger coherent (gun optics aberrations, etc.) contributions to $T_{e\perp}$ could be tuned away by adjustment of the GUN SOLENOID current and the relative potentials of resonant focusing electrodes which surround the beam after the basic diode but before the interaction region.[13]

The mean B_z field direction was adjusted via 5 m long V and H dipole winding pairs, surrounding the interaction region. Local $B_z/|B_z|$ wobble was minimized by constructing the solenoid from 1 meter Al sheet wound segments. The five segments were individually aligned by minimizing the deviatin of a 0.5 mm ϕ test e⁻ beam from a straight line. An rms $B_z \times Z/|B_z| = 4 \times 10^{-4}$ at ≃ 1 cm off axis, corresponding to $T_{e\perp} = 0.039$ ev, was achieved.

Microwave pickup loops were installed next to the e^- beam at one end of the 5 m interaction region in order to directly measure T_{e_1} (∝ magnetic dipole radiation at the cyclotron frequency). Such signals were observed as well as unexpected ones at UHF due to lost electrons oscillating between the gun and collector virtual cathodes. Although used for initial qualitative tuning of the e^- system this diagnostic was not persued during the cooling runs.

The entire e^- beam path is surrounded by drift electrodes, segments of which could be held at portentials appropriate for clearing or trapping ions/electrons. In this way, we were able, for instance, to ensure full radial space charge well conditions (i.e. no neutralization for trapped ions): $\Delta E(r)_{sc} = 30 I_e\{(r_w/a)^2 + 2\ell n\, r_w/a\}/\beta$. This dependence was confirmed by measuring the equilibrium cooled proton beam energy as a function of I_{e^-}. Similar measurements as a function of relative proton/electron beam spatial offset, and other indirect indications were crudely consistant with a homogeneous n. No direct measurement of n(r) was attempted.[11]

3. Cooled Equilibrium

Within a few seconds of their injection protons have cooled such that one observes steady state Schottky bands and transverse profiles: the protons have come into equilibrium with the electron velocity distribution. This is only a quasi-equilibrium since the electron distribution is not (it is replenished to keep it a "disc" - see figure 4). Indeed, we assume here that the frictional and diffusional influence of the electrons are much larger than proton intra beam scattering (IBS) relaxation to true equilibrium.[14] Within the proton current range investigated here there is no evidence of current dependent equilibrium $\delta p/p$.[15] The initial (hot) proton distribution was nearly isotropic ($\delta p/p$ FWHM $\simeq$ 0.17%) and is represented in velocity space in figure 4.

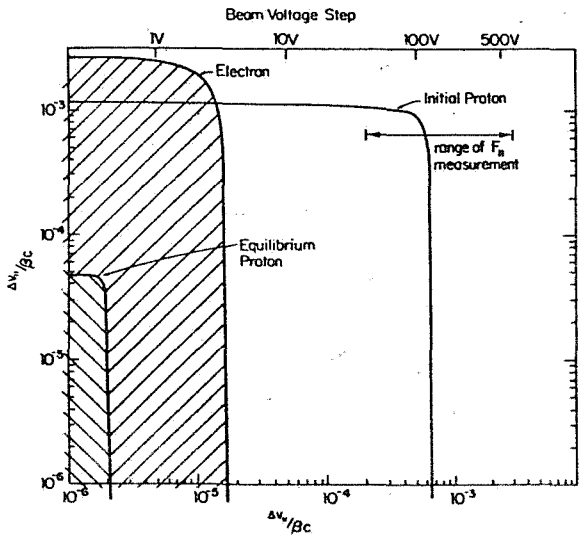

FIG. 4. One σ envelopes of equilibrium velocity distributions. Initial proton and perpendicular equilibrium proton valves are measured. Longitudinal proton equilibrium valve is measured upper limit. Electron values are inferred (see text). Upper horizontal scale is e^- beam voltage (V_o) change needed to produce $\Delta v_{||}/\beta c$ below.

Additionally, there is a mechanism for coherent distortion of the Schottky signals; a freezing out of longitudinal space charge modes on the proton beam above a certain critical current = N_x/T_o.[16] This mechanism can cause a suppression of observed Schottky power density, thus giving a false measure of beam intensity. For our conditions $N_x = 4 \times 10^{12} (\delta p/p)^2 > 10^7$ for even the lowest $\delta p/p$'s observed or expected.

Thus we interpret the Schottky band power spectra area and its FWHM directly as a measure of the beam intensity and momentum spread:

$$\delta p/p_{FWHM} = \eta^{-1}\, \delta f/f_{FWHM} \qquad (2)$$

It was necessary to observe the highest possible (limited by electronics bandwidth) harmonic bands to maximize δf. Even so, the extreme narrowness of the equilibrium bands allowed only an upper limit of 850 Hz FWHM ($\delta p/p = 4 \times 10^{-6}$) to be measured (at 453 MHz; h = 360). This was a consequence of a ±10 V pp residual jitter in the high voltage supply (V_o). In this context it is important to distinguish two cases. Fast fluctuations in V_o contribute only to an effective increase in longitudinal electron temperature $\Delta T_{e_{11}} = \delta V_{rms}^2/(\beta^2\gamma^2 m)$ ($\simeq 5 \times 10^{-5}$ ev for observed jitter). On the other hand slow enough modulation allows the mean proton momentum to be dragged along, in which case the observed Schottky band as a whole will jitter: $\Delta f = \Delta V f \eta/\beta^2\gamma$ ($\simeq$ 25 kHz). Long time average spectra show this 25 kHz envelope, whereas the 0.85 kHz "moving band" measurement sets a ~5 volt rms limit on a fast jitter component amplitude. This is roughly consistant with directly measured longitudinal drag forces (Fig. 5) and observed δV_o time structure.

The projected (horizontal or vertical) transverse proton temperature may be defined at any lattice points as: $T_p(s) = M(\sigma\beta\gamma c/\beta_s)^2$ where β_s is the local beta function and σ is the rms laboratory profile width (horizontal or vertical). Since thermal equilibrium ($T_{p_\perp} \sim T_{e_\perp}$) with the electrons is expected we quote $T_{p_\perp} \equiv T_p(s_e) = T_{p_\perp}(s_{monitor})\,\beta_n/\beta_e$. Our minimum observed $T_{p_\perp} = 0.61$ ev (1-2 amp I_e) = which corresponds to an lab rms angular deviation, $\theta_p(s_e)$, from $B_z/|B_z|$ of 3.7×10^{-5}. As expected from (1) we observed no change in this equilibrium as $B_z/|B_z|$ was varied by $\theta_p\sqrt{M/m}$ (using steering dipoles at s_e).

We summarize the various temperatures measured in figure 4 (using the upper limit $T_{p_{11}}$). The large anisotropy in equilibrium proton v_p distribution is clear evidence for the expected "disc" v_e distribution.[17] However a detailed inference of T_e from T_p requires some model assumptions. In the simplest exact disc ($T_{e_{11}} = 0$, $B_z = 0$) model $T_{p_\perp} = 1/2\, T_{e_\perp}$ (> 0.51 ev minimum cathode contribution).[18,19] Isotropic electrons (still $B_z = 0$) would require $T_{p_\perp} = T_{e_\perp}$ (> 1.02 ev). For B_z such that $r_{larmor} < r_D(B=0)$ (i.e. the maximum initial impact parameter in our case). The full $v_{e_\perp}$ becomes partially decoupled from the friction and diffusion mechanisms. Such "adiabadic" collisions take over entirely in the limit $r_L < n^{-1/3}$, (just satisfied for our data), under the condition of low parallel velocities observed near equilibrium.[20] A more detailed argument suggests $T_{p_\perp,_{11}} \to T_{e_{11}}$ (< 10^{-4} ev!).

We note that no experiments have yet seen this most direct manifestation of "magnetized" cooling, while clear evidence of an adiabadic regime has been found in cooling rates.[17,15] Further confusion comes from anaylsis of recombination (H^o) rate data, which plausibly ought to yield unbiased $v_{e_\perp}$ information (i.e. not dependent on B_z or $f(v_{e_\perp})$).[19,21] We observed H^o rates only during our 114 MeV runs, but due to the extremely low proton intensities involved can only say that they were in agreement with the profilometer $T_{e_\perp}$. This description of adiabadicity assumes perfect alignment of the Larmor "tube" axis with the mean proton velocity (82 Larmor cycles along our full interaction region). Our uncertainty in solenoid alignment and closed orbit centering in the solenoids (the various effects discussed now ideally vanish on axis) allow a Larmor/closed orbit divergence of a few x 10^{-4}. This means that near equilibrium protons diverge $\gtrsim r_L$ ($\simeq n^{-1/3} \simeq r_D \simeq 2 \times 10^{-3}$ cm)[22] over 10 cm of flight path (i.e. only 1.6 Larmor cycles: hardly adiabadic). This divergence, and other transverse drifts (such as ExB space charge precession) also contribute non-adiabadic components to $v_{e_\perp}$, which although small ($\lesssim$ 0.05 eV here), certainly dominate the pure adiabadic value.

A non magnetized expression for equilibrium $T_{p_{11}}$ is[19]

$$T_{p_{11}} = \frac{\pi}{4}\sqrt{T_{e_{11}}\,T_{e_\perp}}\;\; L(v_{e_\perp}/L(v_{e_{11}}) \qquad (3)$$

This gives values only about 25% greater than the more comprehensive result of Sorensen[18] for the conditions of Table 1. Our upper limit $T_{p_{11}}$ value plus $T_e = 2T_p$ yields $T_{e_{11}} \lesssim 0.23\ 10^{-5}$ (+3.6/-0). Notice that $T_{e_{11}}$ determined this way is extremely sensitive, $\propto (\delta p/P\ \text{FWHM})^4$, to the original data to which we assign a + 100% uncertainty. The dominant contribution to $T_{e_{11}}$ in our beam is expected to be from equipartition with Coulomb repulsion: $T_{e_{11}} \simeq e^2 n^{1/3} = 3.7 \times 10^{-5}$ eV.[19] A non magnetized discussion must include IBS amongst electrons, which would create $\Delta T_{e_{11}} = 3.3 \times 10^{-5}$ eV at the interaction center. Although magnetization (again for $r_L \lesssim n^{-1/3}$) should suppress IBS, a large contribution comes from the high n low B_z convergent gun (a distinct disadvantage of this design).

A particular difficulty during these experiments was the lack of good proton beam lifetime, τ_e, with electron beam but not cooling (energies for detuned). Despite extensive "tune point" hunting we were unable to achieve $\tau_e > 40$ sec. for $I_e \geq 1$ amp. Apparently this was due to nonlinear resonance effects of the e^- beam (as a lattice element) since good lifetime ($\geq$ 350 sec) with e^- beam off but all magnetic elements at nominal settings was possible. Our longest observed cooled beam lifetime τ_e, 6200 s, is only ~ 40% less than an estimate based on single coulomb scatter out of the ring acceptance for our mean running vacuum. The vacuum density and composition cancels in the multiple Coulomb scatter τ_e to τ_s ratio, which has been calculated to be 0.076 for the ECR. This yields a τ_e multiple scattering limit of 470s. We attribute our inability to find an adequate operating point to the [for a storeage ring] rather poor lattice magnet current regulation (only 2 x 10^{-4} rms!).

In order to take advantage of the large coherent longitudinal signals possible with RF bunched beams we performed many measurements by a "cooling into buckets" technique, illustrated in figure 5a[23]. Bunch sizes achievable in this way (ideally down to widths $\propto \sqrt{T_{p_{\parallel}}}$ for ω_{RF} tuned to V_o) were limited by only the jitter in V_o (energy detuning) and bend magnet supply (path length detuning). A fixed detuning produces the interesting dynamical equilibrium shown in figure 5b, where the protons circulate around the torus at synchrotron frequency. We observed many detailed manifestations of this behavior. Unfortunately the average cooling friction forces acting on the protons is reduced in proportion to the fraction of torus overlap with the V_o line.

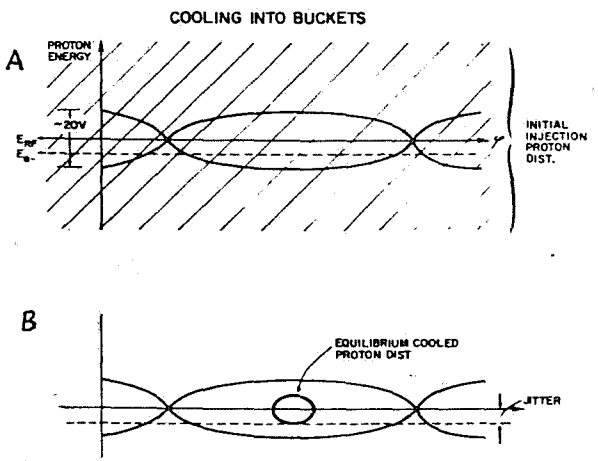

FIG. 5. a) Schematic in longitudinal phase space of "cooling into RF Buckets" TOP: initial proton distribution BOTTOM: equilibrium distribution b) exact 100 particle dynamical simulation showing a steady state arrived at from initial conditions as in a) TOP.

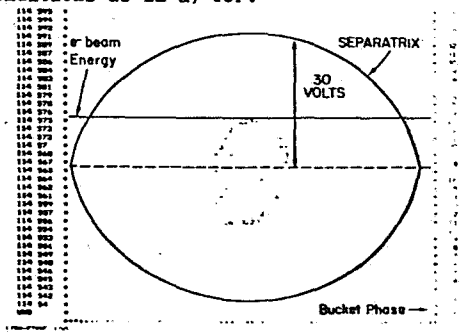

4. Cooling Rates

By instantaneously stepping the e^- beam voltage (ΔV_o) we can follow the history f(t) of a Schottky band peak as it is "dragged" to the new equilibrium point. $F_{\parallel}$ of (1) is then

$$F_{\parallel}(f) = \beta\gamma^m(\delta\eta f)^{-1}\ \frac{\delta f(t)}{\delta t} \qquad (4)$$

Our data is presented in figure 6 as a function of $v_{p_{\parallel}}$ measured from the new electron distribution center and scaled with respect to n, $T_{e_{\parallel}}$ and γ in order to allow comparison with other laboratories (exact for: B = 0, $v_{p_{(1)}} \ll v_e$ and disc distribution). A non magnetized theory (just $\ln$) predicts $F_{\parallel}$ values corresponding to the (typical) L values shown. The curve from a more sophisticated (but still B = 0) treatment agrees well with our data.[18]

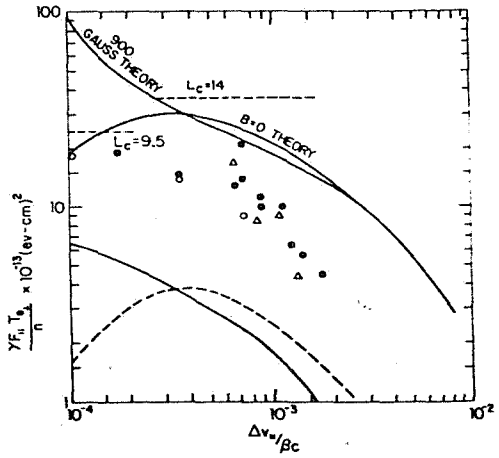

FIG. 6. Scaled longitudinal drag force ($F_{\parallel}$) in moving frame. ●, 114 MeV run. ■,○, Δ, x, 200 MeV run.[11] Lower two curves are CERN (-----) and INP (———) data for comparison.

The simplest magnetized theory (where each collision occurs within ω_p^{-1}) predicts no adiabatic contribution to $F_{\perp}$, under the "drag" experiment condition of $v_{p_\perp} = 0$. However Derbenev and Skrinskii point out[19] that collective (i.e. proton-plasmon processes with the impact parameters in the range $\gtrsim r_p$) collisions, though entering with $L \simeq 1$, can dominate $F_{\perp}$. A full dialectric-plasma description[18] substantiates this conclusion (see Fig. 5), but grossly disagrees with existant data. Such collisions are probably practically ineffective by the same arguement used to explain T_p ($B\rho/\omega_p \simeq 50$ cm)[24]. Novosibirsk data[26] clearly shows evidence of magnetization via its negligible $F_{\perp}$ and H^0 production rate dependence on $T_{cathode}$ (i.e. breaks the scaling used in Fig. 5), which is all the more puzzling given the disagreement of their $F_{\perp}$ with magnetized theory. Our displayed $F_{\perp}$ data represents best tune conditions ($T_{e_\perp} \simeq 1.01$ eV). Evidence from runs with higher $T_{e_\perp}$ (e.g. high I_e) always indicated degraded $F_{\perp}$ values.

We have assumed that the v_p distribution is the same during the drag experiments as it is at their beginning and end points (i.e. equilibrium with v_e). Diffusion (from finite T_e) is negligible. The protons are not damped however, during the drag period. Our severe lifetime limitation in such circumstances leads to considerable beam blow up during draging (indeed we were limited by proton loss to $\lesssim$ 500V steps). Although this may complicate any magnetized theory interpretation ($v_{p_\perp} \neq 0$), it should lead systematically to lowered $F_{\perp}$ values.

Transverse cooling rates were measured by comparing a series of vertical and horizontal profilometer "snapshots" triggered at known times after fresh (hot) proton beam injection. Thus the observed damping is of a beam cooling simultaneously in all three dimensions. figure 7 shows two basic sets of data. The first, from our 114 MeV run which showed evidence of a net B_z, closed orbit misalignment, has a considerably larger damping time than our best results (200 MeV). This is evidence of a "superfast" magnetized cooling effect, since (for the misaligments involved here) nonmagnetized theory predicts a lower rate, independent of angular alignment. Actually the data is clearly not exponential suggesting the need of a complex interpretation which we have not attempted.

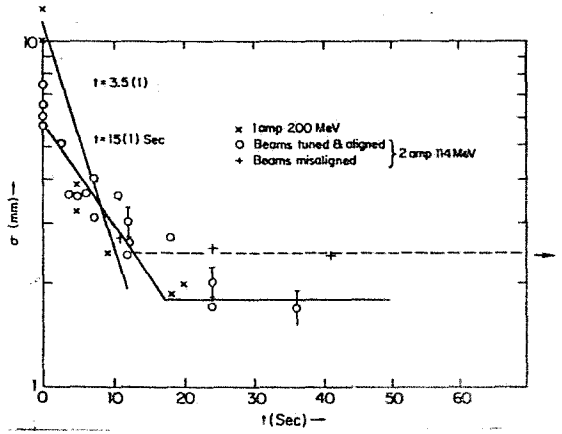

FIG. 7. Verticle proton beam profile width (σ) as a function of time after proton injection into ECR with e^- beam optimally tuned (all 1 amp beam data except as noted).

5. Stacking Studies

The ECR was designed to allow single turn fast kicker injection of fresh (hot) beam while leaving, unperturbed, a cold stack on an outer radius.[7] This is accomplished with two identical full aperture kickers (see Fig. 1) placed symmetrically about the injection point, π phase advance apart, and fired with a relative time delay equal to the transt time between them. Careful chromaticity correction (sextapoles) allowed stable operation over the large ($\simeq$2 %) momentum separation of the two orbits.

Figure 8 shows a preliminary accummulation sequence. In this case the fresh protons were RF captured and accelerated to the cooled stack orbit. An intensity increase of $\simeq$ 12x is shown, which has begun to saturate. The saturation is a result of the anomolously low life time which the stack protons have when they are phase displaced (and thus momentarily not being cooled) by the moving RF bucket. Experiments are in progress to circumvent this problem by turning the bucket off next to the stack and subsequently draging the stack, with an appropriately programmed V_o ramp, to the fresh batch momentum.

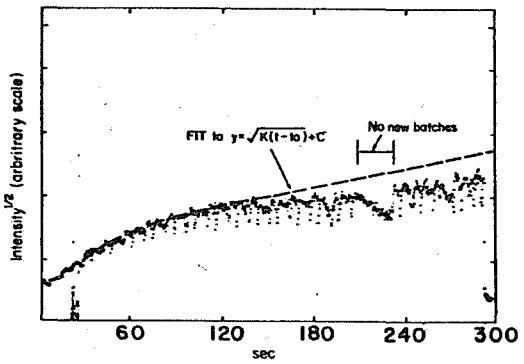

FIG. 8. Accumulation of injected (every ~5 sec., this picture) proton batches into a single cooled core the intensity of which is plotted vs. time. Curve is expected result for no loss accumulation (normalized to first 60 sec.). Notice beam dump 10s from trace end giving zero level.

Acknowledgements

We would like to thank numerous members of the Fermilab Accelerator division staff for continued technical suppport and encouragement. Thanks go also to our collegues at CERN and Novosibirsk who have shared their prior knowledge and results with us at all stages of this work.

References

1. G.I. Budker, et. al., Particle Accelerators 7, 197 (1976)
2. F.T. Cole and F.E. Mills Ann. Rev. Nucl. Part. Sci. 31, 295 (1981)
3. The CERN "ICE", and INP "NAP-M" experiments used up to I_e = 2A, V_o = 26 KeV and $I_e \tilde{=}$1A, V_o = 45 KeV respectively
4. D. Young, Proc. 11th Int. Conf. High-Energy Accelerators, p. 756 (1980)
5. R. Forster, et. al., IEEE trans. Nucl. Sci. NS-28, 2386 (1981)
6. W. Kells, in AIP Conf. Proc. 87, 656 (1981)
7. Fermilab ECR Project Design Report, FNAL (1977) unpublished
8. D. Johnson, 1977 (Aspen) Summer Study, p. 301, edited by J.K. Walker (FNAL, Batavia, Illinois 1977)
9. G.R. Lambertson, IEEE Trans. Nucl. Sci. NS-28, 2471 (1981)
10. T. Hardek and W. Kells, Trans. Nucl. Sci. NS-28, 2219 (1981)
11. T. Ellison, et. al., Fermilab TM-1156 (1983) unpublished.
12. W. Kells, et. al., Fermilab TM-918 (1979) unpublished
13. C. Rubbia, CERN Report EP77-2 (1977) unpublished
14. Ya. S. Derbenev, in Proc. 6th All Union Conf. High Energy Particle Accel., Dubna (1978).
15. M. Bell, et. al., Nucl. Inst. Meth. 190, 237 (1981). See also A.N. Skrinskii and V.V. Parkhomchuck, Fiz. Elem. Chastits. At. Yardr 12, 557 (1981).
16. V.V. Parhomchuck and D.V. Pestrikov, Sov. Phys. Tech. Phys. 25, 818 (1980)
17. N.S. Dikansky, et. al., INP preprint 79-56 (1979) unpublished. See also Ref. 15 and 14.
18. A. Sorensen and E. Bonderup, to be published Nucl. Phys. B. (1982)
19. Ya. S. Derbenev and A.N. Skrinskii, Fiz. Plazmy, 4 492 (1978)
20. The adiabadic condition is that $\tau_{collision} \geq \Omega^{-1}$ cycl. But: $\tau_{coll} = r_{min}/u > r_{min}/V_{e_\perp} > r_{L_\perp}/V_{e_\perp} \equiv \Omega^{-1}$ cycl. where r_{min} = minimum impact parameter (> $n^{-1/3}$).
21. MainBell, and J.S. Bell, CERN Report TH-3054 (1981) unpublished.
22. The effective temperature for r_D here excludes any V_e contribution since transverse motion is constrained by B_z
23. W. Kells, Fermilab TM-1153 (1982) unpublished.
24. A general condition for effective adiabadic collisions is that $\Omega_{cycl}/\omega_p >> 1$ which is well satisfied in our case (10:1) see Ref. 18.